CHAPTER 5. RELIABILITY-BASED DESIGN OPTIMIZATION OF AIRPORTS CONCRETE PAVEMENT

Adel Rezaei Tarahomi, Ramin Giahi, Cameron MacKenzie, Halil Ceylan, Sunghwan Kim, Kasthurirangan Gopalakrishnan

Modified from a manuscript to be submitted to the International Journal of Pavement Engineering

Abstract

The current state-of-the-art airfield concrete pavement design is accomplished using FAARFIELD software developed and released by the U.S. Federal Aviation Administration (FAA). Since this mode of design is implemented based on some initial assumed inputs, obtaining an optimum design for a given traffic and environmental loading and design age is an iterative process to find the best possible design. However, it takes considerable amount of time to perform this iterative process using the 3-D Finite Element (FE) based FAARFIELD software. To overcome this challenge, a more efficient methodology, Simulation Optimization for Airfield Rigid Pavement (SOARP), is proposed. SOARP relies on artificial neural network (ANN) models combined with a design optimization framework to determine the optimal design of airfield rigid pavement, and this optimal design should perform satisfactorily for different values of uncertain parameters. SOARP is implemented for various reliability levels and design lives for the airfield rigid pavement. In addition, the pavement thickness designed by SOARP and FAARFIELD are compared for various flexural strength and reliability levels. The results show that SOARP either results in more reliable or less expensive pavement designs.

Introduction

Airport pavements are designed over many years to withstand repeated traffic loading imposed by a broad entire range of aircraft types over many years, to resist the abrasive action of traffic, and to endure deterioration induced by adverse weather conditions (e.g., extreme hot or cold weather) and other influences in a cost-effective manner. For rigid airport pavement design, the Federal Aviation Administrative (FAA) uses three-dimensional finite- element (3D-FE) procedures for rigid airport pavement design, as implemented in the FAA Rigid and Flexible Iterative Elastic Layer Design (FAARFIELD) program [1]. The iterative processes encountered in rigid pavement thickness design based on 3D-FE solution exhibit long and unpredictable run times, especially when the number of slabs is increased and top-down cracking is considered [2]–[6].

Although there are many features affecting pavement performance, typical airfield rigid pavement design processes in FAARFIELD use a trial-and-error approach to find optimum slab size (joint spacing), joint stiffness, temperature-induced initial curling, and predefined load location, using a trial-and -error approach. Since it is also not practical to determine the optimum design solution from an exhaustive set of all acceptable designs using this approach [7], some practical alternatives are needed to expand the airfield rigid pavement design beyond the current restricted approach, making design calculation computationally-tractable, agile, and comprehensive. To achieve this goal, this study proposes a novel approach utilizing Artificial Neural Networks (ANN) along with an optimization technique for airfield rigid pavement design, recognizing that there have been previous studies utilizing predictive models (e.g., ANN) or optimization methods in pavement design and rehabilitation problems to make pavement engineering practices versatile and practical.

Santos and Ferreira [8] presented a deterministic pavement-design optimization model that considers pavement performance, construction costs, maintenance and rehabilitation costs in the model, assuming deterministic values for all model parameters. Mikolaj, et.al., [9] optimized a rehabilitation plan featuring cost-benefit analysis to maximize life-cycle length of pavement constructed with asphalt concrete materials. Hadi and Arfiadi [10] used a genetic algorithm to optimize pavement building costs of rigid highway pavement. Mamlouk et al. [11] developed a project-level optimization model for flexible pavements whose design variables were initial pavement thickness, overlay thickness, and overlay timing used to minimize highway agency and user costs.

Engineering design problems typically have multiple variables, and there is often uncertainty around these variables [12]. Monte Carlo simulation is often used to explore the design output given design parameters [13]. Some studies in the pavement design area have considered that simulation evaluates the effects of different design inputs on the desired output [14]–[16]. For example, Timm & Newcomb [14] developed a Monte Carlo simulation framework for asphalt to conduct a probabilistic analysis of pavement reaction to loading and to evaluate the resulting damage. In their proposed framework, to meet the damage criteria, random samples were generated from probability distributions of asphalt layer thickness, loading configurations, and material properties, and sequences of new random numbers were generated from the input parameters until the level of damage is less than a threshold value. Their proposed frameworks lack an optimization model that could lead to an exact or near-exact solution.

Design of new and rehabilitated pavements involves many uncertainties, variabilities, and approximations. Generally, reliability refers to the ability of the system to perform above

a safety limit under various sources of uncertainty [17]. In pavement design, reliability can be defined as the probability that pavement performance would remain within an allowable range during the design life [18]. A reliability-based pavement design can properly incorporate the uncertainty and variability to make an effective design [19], [20]. The American Association of State Highway and Transportation Officials (AASHTO) mechanistic empirical pavement design guide (MEPDG) considers the reliability of pavement sections in the design [18]. Dinegdae et al. [18] evaluated pavement reliability analysis by incorporating response surface methods. They developed a two-component reliability analysis methodology to evaluate the reliability of fatigue cracking failure in actual field pavements. Their study shows how the influence of different design input variables can be captured within a reliability analysis framework. Retherford & McDonald [21] investigated potential reliability methods and discussed their advantages and disadvantages in the mechanistic empirical design approach to pavement design.

A number of studies applied reliability in the pavement design optimization. Sanchez-Silva et al. [22] presented a model for reliability cost-based optimization of asphalt pavement structures that considered asphalt-surface fatigue damage and the degradation of granular materials by repetitive loading cycles. They also combined reliability-based design optimization with long-term pavement-maintenance policy. Gaurav et al. [7] minimized asphalt-pavement design costs using a surrogate-based optimization approach. They considered design reliability in the model via the use of chance constraints, and the design variables were the asphalt-concrete base, and sub-base thicknesses. They considered deterministic values for model parameters such as Granular base, Granular sub-base, and sub-grade. By considering different reliability levels in pavement design optimization,

decision makers can determine an optimal design that considers expected design costs or choose a design that meets their degree of risk aversion.

The objective of this study is to develop a novel design methodology called Simulation Optimization for Airfield Rigid Pavement (SOARP). SOARP is a comprehensive reliability-based simulation-optimization framework benefiting from artificial intelligence for critical stress responses prediction for the airfield concrete design. The optimal design can be identified more quickly than with other methods. This framework empowers the designers to consider large number of scenarios for designing airfield concrete pavement. This study proposes SOARP for decision makers involved in the design of airport concrete to achieve various reliability levels. The novelty of this study and its primary difference with FAARFIELD's design methods lie in its use of ANN to predict critical responses. Another difference is to conduct airfield concrete pavement design with using Monte Carlo simulation and Bayesian optimization under different reliability levels.

ANN-based Bayesian Optimization Framework

Figure 5.1 shows the whole procedures of the SOARP Framework. The framework is aimed at minimizing the design cost while the fatigue failure of the pavement is kept under the allowable amount by a reliability constraint. The cost function (objective function) represents the total cost of the design thickness of the Portland cement concrete (PCC) slab, base layer, and subbase layer. The reliability constraint limits structural fatigue life of the pavement to an allowable load repetition-to-failure using the cumulative damage factor (CDF). The CDF calculation follows the same method used in FAARFIELD [1], [23], [24]. Unlike FAARFIELD, an ANN is used instead of finite element analysis to determine the critical response. SOARP employs ANNs as analysis engine for replicating critical stress responses associated with cracking which is used for calculating the CDF of the pavement.

Using an ANN in this framework enables performing large number of simulations without interruptions induced by time-consuming analysis and complex calculations.

The following subsections describe the approaches, models, and the mathematics employed for design optimization including CDF calculations, reliability constraint, objective function, ANN models development, and Bayesian optimization algorithm.

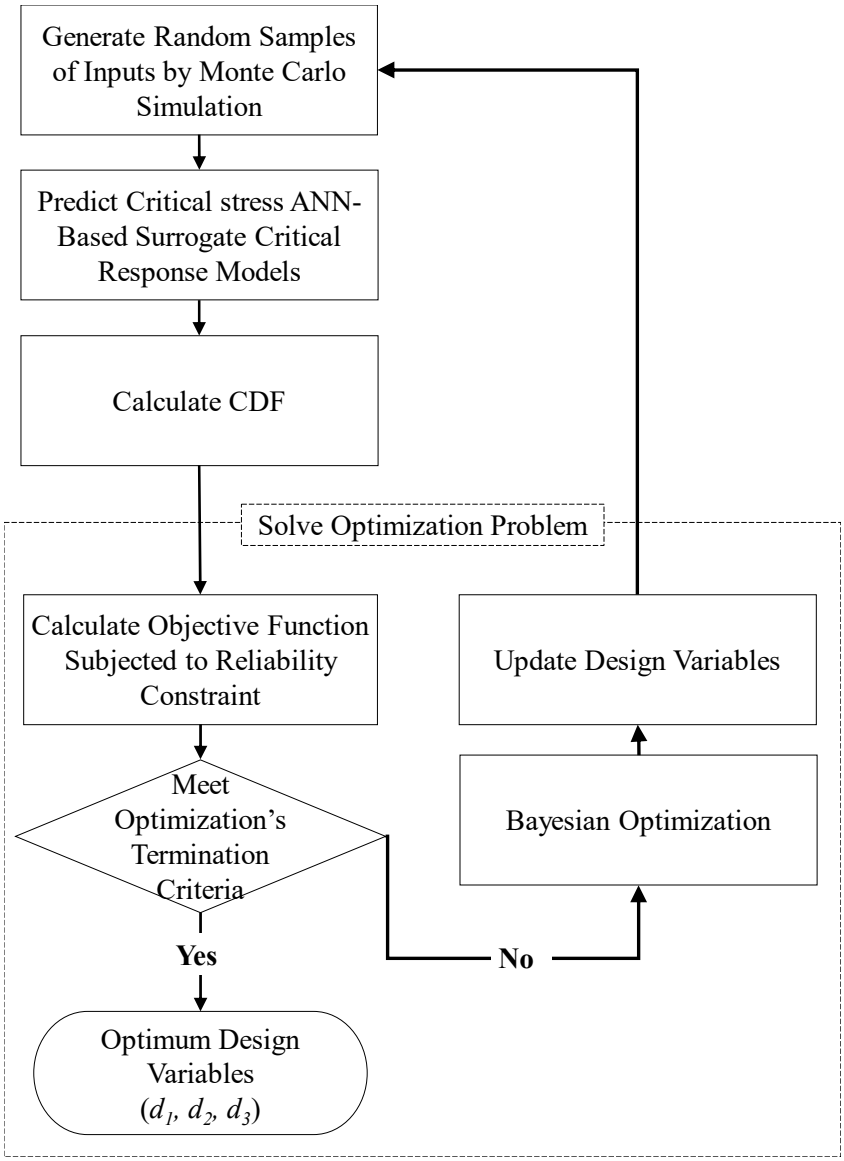

Figure 5.1 *Flow chart of the SOARP steps.*

Mathematical Model

This section describes the approaches, models, and the mathematical methods employed for design optimization, including total damage caused by an aircraft traffic mix, an objective function, and a design cost function. The objective function limits the structural fatigue life of the pavement to allowable load repetition-to-failure using cumulative damage factor (CDF). The cost function represents the total cost of the design thickness of the PCC slab, base layer, and subbase layer. In this study, design optimization was aimed toward minimizing design cost while using a reliability constraint to keep pavement fatigue failure below a tolerable level, using the same method of fatigue life calculation used in FAA rigid airfield pavement design software (FAARFIELD) [23], [24].

The proposed design method followed the following steps:

1. Randomly generate *N* samples from the distributions of uncertain parameters: Gear loading angle (θ_g), Loading location on the slab (X and Y), temperature gradient, thermal coefficient, PCC slab cost, base layer cost, and subbase layer cost.

2. Calculate critical bottom tensile stress using the trained ANN models for the airplanes (see CHAPTER 3).

3. Calculate cumulative damage factor [1] for each airplane using the design variables (PCC slab thickness (d_1), base layer thickness (d_2), and subbase layer thickness (d_3)) by the optimization algorithm:

$$CDF = \frac{(\text{annual departure}) \times (\text{life in years})}{(\frac{\text{pass}}{\text{covrage ratio}}) \times (\text{covergae to failure})} \tag{5.1}$$

To calculate the pass-to-coverage ratio (P/C), coverage-to-pass (C/P) is calculated using Equation (5.2. For rigid pavements, the pavement surface is divided into 81

longitudinal strips (10-inch strips at lateral distance between -400 and 400 in.), and the C/P ratio is computed for each offset. For each offset i, $(C/P)_i$ is computed using the following probability equation:

$$(C/P)_i = \sum_{k=1}^{N_t} P\left[\left(x_i - \frac{w}{2}\right) \le x_k \le \left(x_i + \frac{w}{2}\right)\right] \tag{5.2}$$

where N_t is the number of tires on the landing gear, x_i is lateral distance from a longitudinal reference line (e.g., runway or taxiway centerline) to the midpoint of strip i, x_k is the lateral distance from the same reference line to the centerline of tire k [24], and w is tire width. Coverage to design failure (C) can then be obtained by solving Equation (5.3 [23]:

$$DF = \left[\frac{F_s' bd}{(1-\alpha)(d-b) + F_s' b}\right] \times \log C + \left[\frac{(1-\alpha)(ad-bc) + F_s' bc}{(1-\alpha)(d-b) + F_s' b}\right] \tag{5.3}$$

where the design factor $DF = R/\sigma$ and $\alpha = SCI/100$. R is the flexural strength of the PCC and σ is the analytical stress obtained by ANN critical response models. For new rigid pavements, a structural condition index (*SCI*) of 80 is the FAA definition of structural failure, consistent with the condition that 50 percent of slabs in the traffic area exhibit a structural crack [25]. The parameter values of Equation (5.3 from Brill and Kawa [26] are:

$$\begin{aligned} F_s' &= 1 \\ b &= d = 0.160 \\ a &= 0.760 + 2.543 \times 10^{-5}(E - 4500) \\ c &= 0.857 + 2.314 \times 10^{-5}(E - 4500) \end{aligned} \tag{5.4}$$

where E is the subgrade modulus considered to be 20,000 psi in this chapter. To calculate the cumulative CDF (CCDF), the CDF values for all airplanes in the traffic mix load are

summed for each of the 81 strips, after which the peak value of the CCDF is represented as TCDF (Equation (5.3). Figure 5.2 shows the CCDF and CDF values calculated by Equation (5.1 for each airplane.

$$CCDF_s = \sum_{k=1}^{4} CDF_{ks} \qquad \forall s = \{1, 2, ..., 80\}$$
$$TCDF = \max_s CCDF_s \tag{5.5}$$

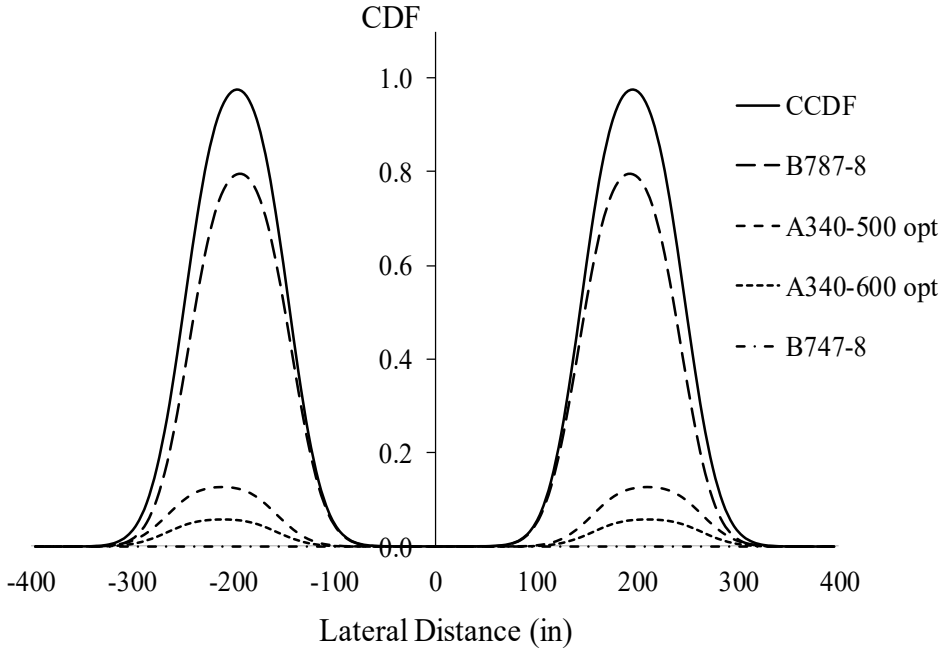

Figure 5.2 *CCDF and the CDF for each airplane.*

4. Solve the optimization problem and use MSC to determine the expected design cost, while ensuring that the reliability constraint is not violated:

$$\underset{d \in D}{\text{minimize}} \ \frac{1}{N} \sum_{j=1}^{N} \sum_{q=1}^{Q} C_{jq} d_q$$
$$\text{subject to } P\left(TCDF \le T\right) \ge \Re \tag{5.6}$$

The first part of Equation (5.6) represents the expected design cost considering N simulations, where C_{jq} is the cost of design for design variable d in simulation j. Since several of the parameters are uncertain, Monte Carlo simulation can be used to calculate the cost function, with the expected cost of design calculated as the average after N different simulations. The second part of Equation (5.6) shows the reliability constraint representing the simulated probability that TCDF is less than or equal to T (e.g., 1.05), where T is the TCDF threshold.

The decision maker establishes reliability level $\Re$ (e.g., 0.95) before optimizing the problem using Equation (5.6). For a design to be reliable, the TCDF should be less than the threshold (T) $\Re$ % of the time. This framework allows the design to fail fewer than $(1-\Re)$ % of the time. If $TCDF > T$ the pavement will fail before reaching its design life, but it would be too costly to build or design a system that would never fail during its operation.

The Bayesian optimization algorithm is used to solve this problem. The algorithm procedure and the optimization termination criteria are elaborated in detail in Optimization Algorithm section.

Artificial Neural Networks

Previous chapters showed that employing ANN in the current FAA design process can be beneficial by performing rapid analysis and reducing computer run time for multiple-slab simulation to a matter of seconds. Incorporating ANN surrogate response models into the pavement design process can therefore significantly enhance efficiency of the design process by reducing the iteration time for calculation of critical stresses for each type of aircraft in a mixed-aircraft traffic loading scenario. Using rapid-response ANN models can

also help expand current design method beyond those compromising the currently used one-slab model involving limited-loading circumstances.

Before incorporating such alternative models into the current FAA design process, they must be tested and validated. Chapter I assesses ANN models accuracy in analyzing airfield concrete pavement using various testing, independent testing, and sensitivity testing data sets. The accuracy metrics demonstrated promising predictions for training and testing and confirmed a good fit and a lack of memorization of the predictors-output relationship. In addition, this study is presenting SOARP method which employs the trained ANN models along with the FAA's airfield concrete pavement design. This method enables finding the optimum thickness for each pavement's layer by using the ANN-predicted critical stress. Moreover, it is implemented in a case study and then validated by comparing SOARP method with FAARFIELD.

Optimization Algorithm

In this study, the expected cost of design is minimized under different reliability levels. To calculate the objective function and determine an optimal design, the ANN model is used in each simulation scenario. ANNs are complex black box functions whose outputs provide little information about functional forms because there is often no simple relationship between network weights and model properties [27]. The first or second order information of the highly nonlinear simulation model is hard to estimate. Hence, the traditional optimization algorithms such as gradient descent which uses the first order information of the objective function is not applicable to solve the problem. The Bayesian optimization is able to achieve accurate results in reasonable time compared to other optimization algorithms such as random search and evolutionary algorithms [28]. This algorithm outperforms other global optimization algorithms on challenging optimization problems [29].

Bayesian optimization algorithm can effectively model input-output relationships of a black-box model. The inputs of the model are the design variables and the outputs are the design costs evaluated with the Monte Carlo simulation. As the procedure to calculate the design is complex and consist of uncertain parameters, the design cost can only be evaluated with the Monte Carlo simulation. Considering uncertainty in the parameters in the pavement design frameworks requires the use of computationally expensive simulations to evaluate and calculate the objective function. Bayesian optimization generates candidate designs and inserts them into the model and then evaluates the resulting objective function to minimize expected cost. This algorithm constitutes a powerful method for finding the optimal design d^*. The Bayesian optimization algorithm creates a surrogate model for the objective function and exploits it in order to find the next evaluation points in the feasible solution space [30]. The Gaussian process is a powerful prior distribution for functions; therefore, we select it as the prior over the objective function [29]. Bayesian optimization estimates the objective function using J samples of the design variables d. The algorithm fits a prior multivariate normal with a mean of 0 and covariance matrix K over the J samples. After simulating J design alternatives to estimate $f_{1:J}$ - the expected cost assuming the J design alternatives - the posterior mean and variance of a new design alternative d' can be calculated using the Sherman-Woodbury-Morrison formula:

$$\mu(d' \mid d_{1:J}) = k(d', d_{1:J}) K(d_{1:J}, d_{1:J})^{-1} f_{1:J} \tag{5.7}$$

$$\sigma^2(d' \mid d_{1:J}) = k(d', d') - k(d', d_{1:J}) K(d_{1:J}, d_{1:J})^{-1} f_{1:J} \tag{5.8}$$

where $d_{1:J}$ is the J previously evaluated thicknesses used to predict the next point. The objective function at the new design alternative d' has the following form:

$$f(d'\,|\,d_{1:J}) \sim N\left(\mu(d'\,|\,d_{1:J}), \sigma^2(d'\,|\,d_{1:J})\right) \tag{5.9}$$

Bayesian optimization selects the $J+1$ design variable by maximizing the following utility (i.e., acquisition) function:

$$u(d^{'}\,|\,S_{1:J}) = E(\max\{0, f_{J+1}(d) - f(d^{+})\}\,|\,S_{1:J}) \tag{5.10}$$

where $d^{+} = \arg\max_{d \in \{d_{1:J}\}} f(d)$ is the current best design that results in the smallest expected design cost based on J evaluated alternatives. The set $S_J = \{d_{1:J}, f_{1:J}\}$ contains J design alternatives and their corresponding expected costs assessed via simulation. Maximizing the acquisition function represents a trade-off between exploration and exploitation. When the algorithm chooses to exploit, it seeks to sample in solution spaces close to designs that already generate small expected costs. However, when it explores the solution space it chooses to simulate a design alternative with a larger uncertainty [31]. This procedure iterates until there is very little improvement in the objective function or the maximum number of iterations I is reached (i.e, termination criteria) [32], [33]. Algorithm 1 describes the Bayesian optimization procedure. The implementation procedure is adopted from the Random Embedding Bayesian Optimization (REMBO) algorithm developed by Wang et al. [34].

Algorithm 1 Implementation procedure of Bayesian optimization

1: **for** $i = 1$ to I **do**
2: Calculate $\mu(d^{'}\,|\,d_{1:J})$ and $\sigma^2(d^{'}\,|\,d_{1:J})$
3: Find d_{J+1} by optimizing the acquisition function
$u(d^{'}\,|\,d_{1:J}) = E(\max\{0, f_{J+1}(d) - f(d^{+})\}\,|\,d_{1:J})$
4: Use Monte Carlo simulation to calculate $f(d_{J+1})$
5: Augment data points $S_{J+1} = S_J \bigcup \{(d_{J+1}, f(d_{J+1}))\}$
6: **end for**

7: $d^* = \arg\max f(d_{1:J})$

8: Output: d^* : Optimal design variables (slab, base, and subbase thickness)

Pavement Design Optimization Case Study

The case study described in this section involved design of a nine-slab concrete pavement with base and subbase layers on top of a subgrade. Aircraft traffic assumed in this study included a B747-8, a B787-8, an A340-500 opt, and an A340-600 opt with 3,000, 3,000, 1,500, and 1,500 annual departures, respectively. The costs used for this case study were those for designing an airport in Des Moines, Iowa. [35].

Table 5.1 describes the parameters of the model along with the values used in the case study [35].

Table 5.1 *Input values used for the case study.*

Inputs		**Value**
PCC Slab	Modulus (psi)	3.0×10^6
	Poisson Ratio	0.15
Base	Modulus (psi)	5.0×10^5
	Poisson Ratio	0.2
Granular Subbase	Modulus (psi)	7.5×10^4
	Poisson Ratio	0.35
Subgrade	Modulus (psi)	2.0×10^4
	Poisson Ratio	0.4
Slab Dimension (ft.)		20×20
Loading Angle Θ_g (degree)		*Uniform*(5, 85)
Loading Position X		*Triangular*(0.47, 0.85, 1)
Loading Position Y		*Triangular*(0, 0.4, 0.5)
Temperature Gradient (°F/in.)		*Normal*(0, 0.65^2)
Thermal Coefficient (1/°F)		5.1×10^{-6}
Equivalent Joint Stiffness (psi/in)		1.0×10^5
Concrete Strength (psi)		650

PCC Cost (6") (Sq. Yd.)	*Uniform*(55, 80)
Base Layer (6") (Sq. Yd.)	*Uniform*(20, 30)
Subbase layer (6") (Sq. Yd.)	*Uniform*(9.5, 14.5)

Based on the probabilistic distributions of uncertain parameters, 10,000 samples (enough for pavement design [14]) were generated using Monte Carlo simulation. Samples generated by the Monte Carlo simulation are then entered the ANN models to estimate the critical stress in the PCC slab.

The distribution of *TCDF* is estimated from 10,000 simulations of the inputs. If the design variables generated by algorithm 1 ensure that the reliability constraint is met, the expected cost would be recorded for that design (Equation (5.6), and this process is iterated until the optimization termination criteria has been met.

Table 5.2 shows the optimal design for different design life and reliability levels. For lives of 20, 25, and 30 years, a higher level of reliability is associated with thicker concrete pavement structure and consequent higher expected cost. For example, for a 20-year design life and 50% reliability, the total thickness is 38.3 in, while for 95% reliability it is 49.4 in., reflecting a 25% increase in the expected design cost. Figure 5.3 illustrates the rising trend in expected cost when the design life increases from 20 to 30 years and the reliability level increases from 50% to 95%.

Figure 5.4 shows the *TCDF* distribution (for 10,000 different combinations of inputs) of the optimal designs for a 20-year design life at various reliability levels. For example, the 0.95-reliability plot implies that, for 10,000 simulations, 9,500 of the designs meet the reliability constraint ($TCDF <= 1.05$). The pavement structures with the calculated optimum thicknesses withstand applied traffic and environmental loading during a 20-year design life without reaching the maximum fatigue damage level caused by the loading.

Table 5.2 *Optimal thicknesses for different design lives and reliability levels.*

Design Life	Reliability	Thickness (in)			Expected Cost
		Slab	Base	Subbase	
20	0.50	15.8	16.5	6.0	$11,446
	0.80	15.5	21.9	6.0	$12,310
	0.90	15.2	24.6	6.0	$12,642
	0.95	13.4	30.0	6.0	$12,784
25	0.50	15.9	16.2	6.0	$11,479
	0.80	15.4	22.2	6.0	$12,335
	0.90	14.6	26.7	6.0	$12,742
	0.95	13.6	30.0	6.0	$12,853
30	0.50	15.9	16.7	6.0	$11,565
	0.80	14.9	24.1	6.0	$12,422
	0.90	15.2	25.1	6.0	$12,765
	0.95	13.7	30.0	6.0	$12,951

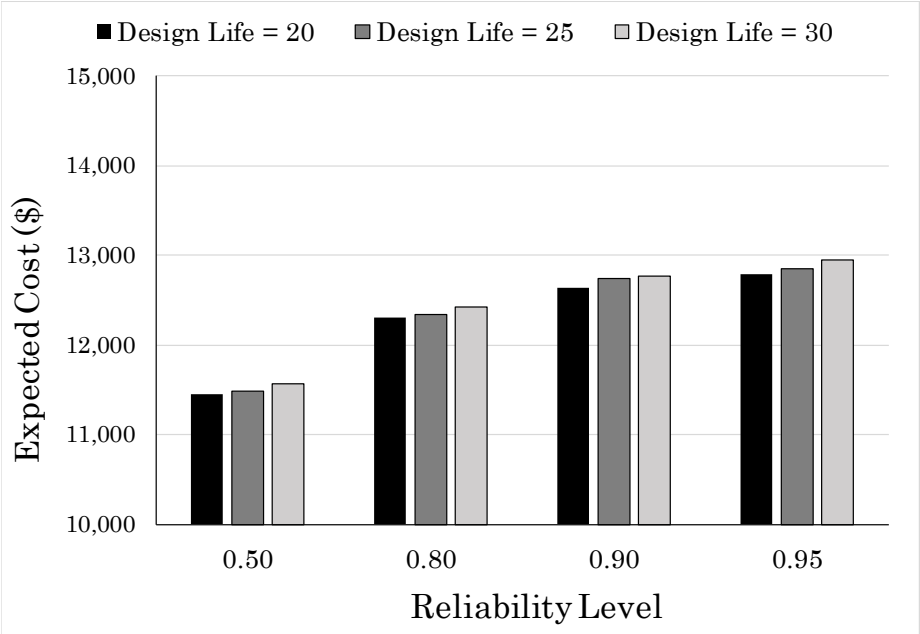

Figure 5.3 *Expected cost variation for different reliability level and design life.*

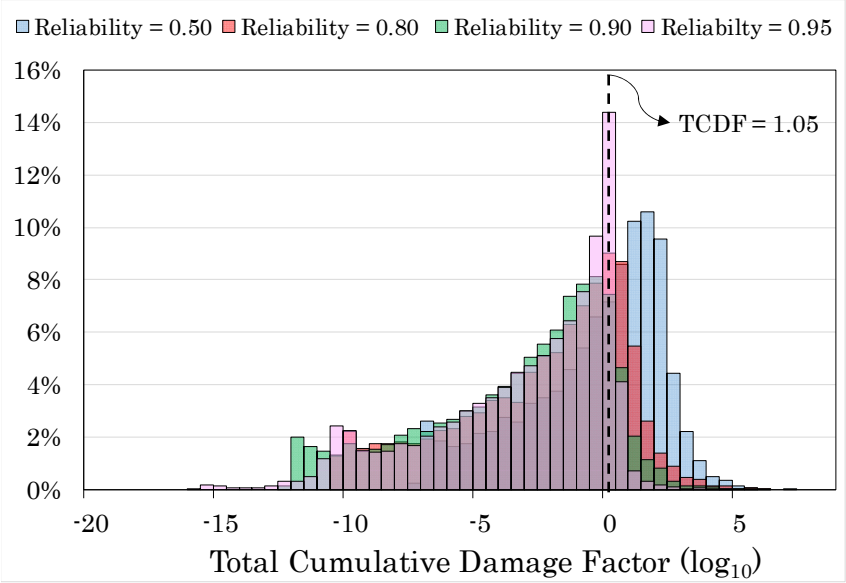

Figure 5.4 *The distribution of TCDF value for optimal design of 20 years design life.*

The expected cost for the optimal design at given different reliability levels and design lives are reported in Table 5.2. Figure 5.5 shows the distribution of the cost for the optimal design of the concrete pavement for 95% reliability and design life of 20 years. The figure shows that there is approximately a 90% probability that the design cost will be between \$10,951 and \$14,612 per 20×20 $ft.^2$ slab.

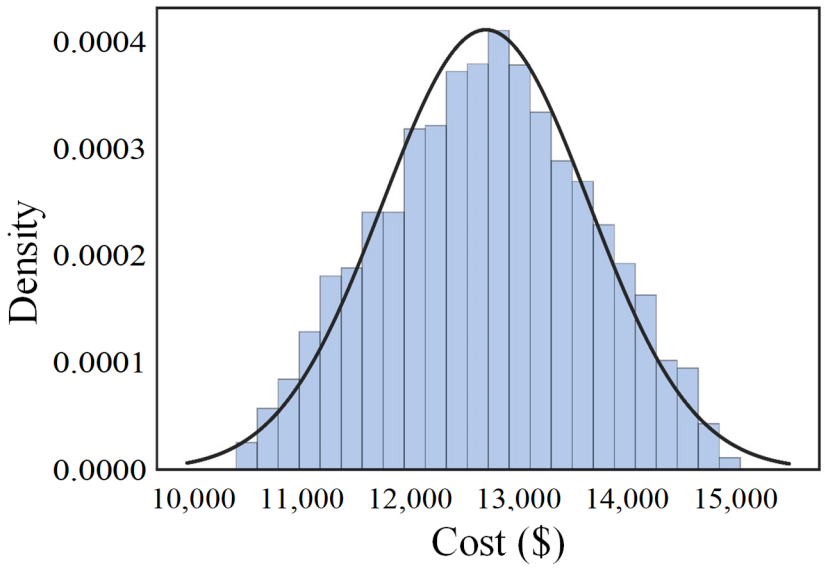

Figure 5.5 *Cost distribution of optimal design for reliability = 0.95 and design life = 20.*

Sensitivity Analysis

The sensitivity of the pavement thickness design to the PCC and subgrade elastic modulus variation will be demonstrated in this section. Although PCC and subgrade modulus were both considered constant, they are very effective in determining the responses and consequent design outcomes.

Sensitivity of total thickness to PCC flexural strength

Figure 5.6 is presented to illustrate the designed total thickness including PCC thickness (d_1), base layer thickness (d_2), and subbase layer thickness (d_3) for different PCC flexural strength values. In addition, Figure 5.6 displays the expected cost variation for various optimal design of SOARP obtained for different flexural strength. The figures show that increasing the strength of the PCC slab results in lower expected cost and total thickness ($d_1+d_2+d_3$) for the optimal designs. For example, increasing the flexural strength from 650 to 800 psi reduces the expected cost of a 20×20 ft slab from \$16,230 to \$11,760.

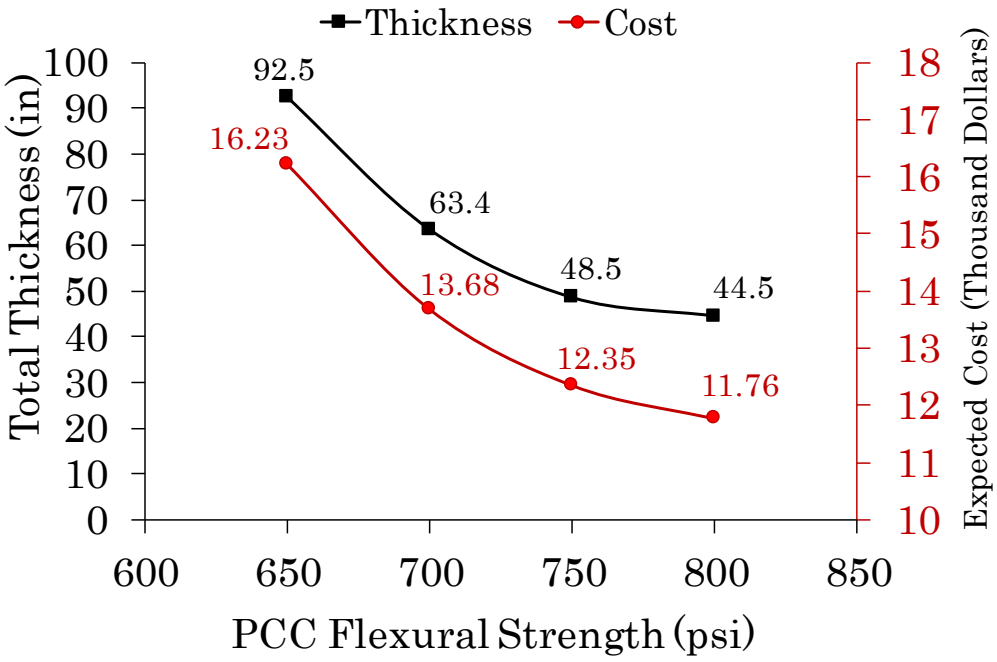

Figure 5.6 *Sensitivity analysis for PCC slab elastic modulus.*

Sensitivity of PCC thickness to subgrade elastic modulus

Figure 5.7 displays the optimum PCC thickness variation for various subgrade modulus. Figure 5.7 shows that increasing the subgrade strength will decrease the optimum PCC thickness, leading to the conclusion that stronger subgrades can afford to have thinner PCC slabs on them to be protected from load-induced deterioration. Also Figure 5.7 shows decrease of the expected cost when subgrade elastic modulus increases. In this study, variation of the subgrade modulus directly affects on critical stress occurred in the PCC slab. Higher elastic modulus results in lower critical stress and consequently lower required thickness.

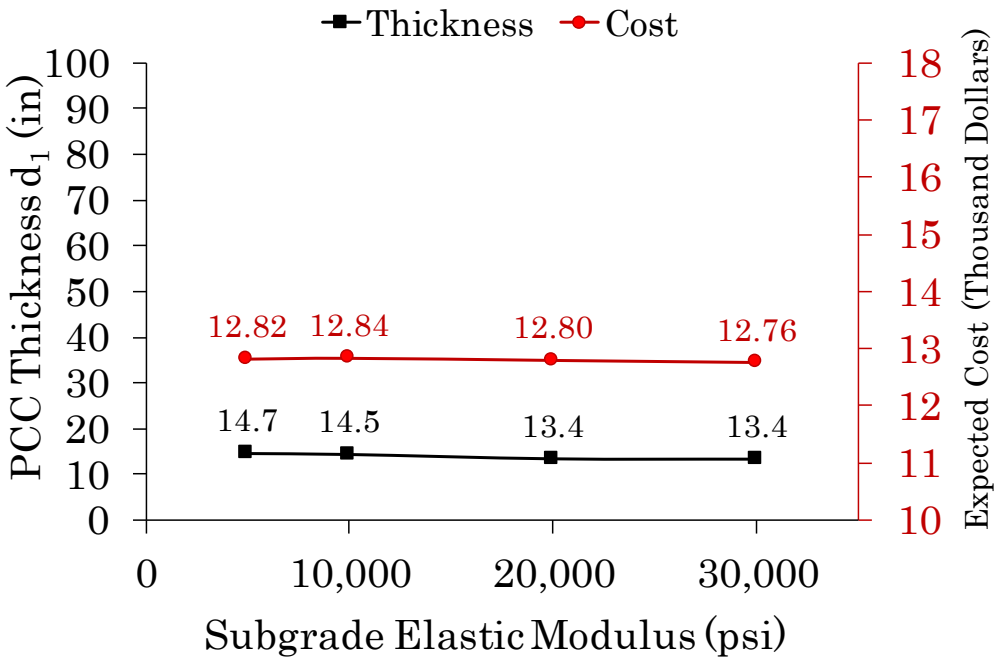

Figure 5.7 *Sensitivity analysis for subgrade elastic modulus.*

Design with FAARFIELD vs SOARP

This section compares results from the proposed design framework with those from the FAARFIELD design. FAARFIELD receives design inputs and determines the PCC slab thickness that results in CDF=1 for a given design life and traffic mix. FAARFIELD

considers the critical condition of edge loading when determining the PCC slab thickness. However, the proposed model considers 10,000 scenarios for the uncertain parameters and considers them all in the process of optimizing the thickness leading to consideration of many critical or non-critical conditions either in simulation or optimization. The proposed design has considered all possible conditions that could possibly affect the pavement.

The SOARP method is used to calculate the optimal PCC slab, base, and subbase thickness for different levels of flexural strength of the PCC. These thickness values for the base and subbase layers are used in FAARFIELD to calculate the slab thickness while assuming the same traffic loading mix, layer properties, and design life. Figure 5.8 shows FAARFIELD's design for $R = 700$ psi and reliability = 50% for a given base and subbase thickness determined with SOARP.

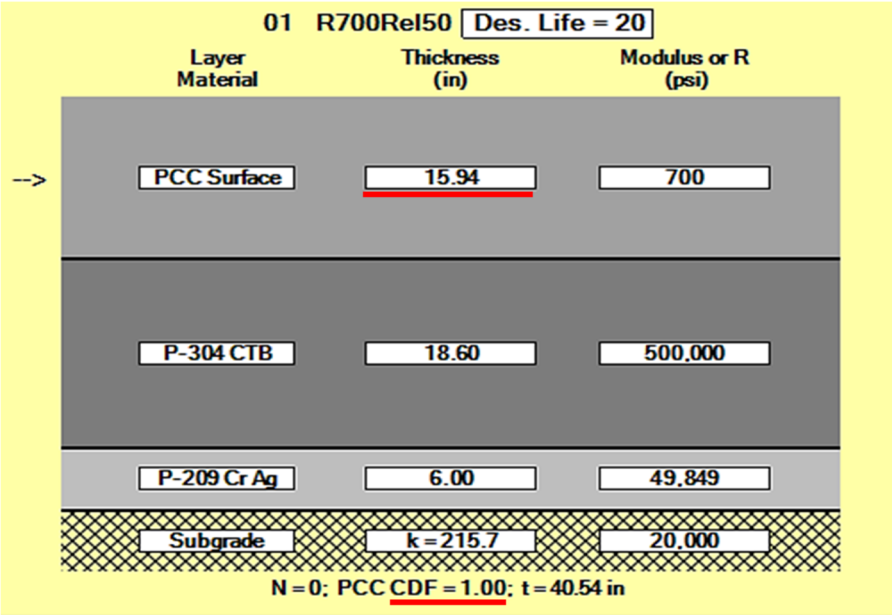

Figure 5.8 *FAARFIELD software's design thickness.*

Figure 5.9 compares the slab thickness calculated by FAARFIELD to that found by SOARP when flexural strength of the PCC slab is changed. Figures 5.9 (a) and 5.9 (b) display the PCC thickness corresponding to obtained reliabilities of 50% and 95%,

respectively. For a reliability of 50%, while FAARFIELD's designed PCC thicknesses is higher than those of SOARP's results except for $R = 800$. For a reliability of 95%, SOARP's optimal PCC thicknesses are higher than FAARFIELD's designed thicknesses. This suggests that if FAARFIELD's designed slab thickness is used in SOARP's framework the obtained reliability would likely be more than 50% and less than 95%. For example, when FAARFIELD's designed thickness of $d_1 = 15.9$ ($d_2 = 19$ and $d_3 = 6$) is used in 10,000 simulations of the SOARP, nearly 63% of them resulted in $TCDF <= 1.05$, corresponding to reliability of 0.63 (see Figure 5.9 (a)). Also, when FAARFIELD's designed slab thickness of $d_1 = 11.5$ ($d_2 = 30$ and $d_3 = 21$) is used for SOARP simulation, 70% of the simulations resulted in $TCDF <= 1.05$ (reliability = 0.7) (see Figure 5.9 (b)). It is indicating that FAARFIELD either recommends a more expensive design when there is a 50% reliability, or it recommends a design that does not achieve the 95% reliability. As the reliability increases, SOARP design tends to result in thicker PCC slabs than for FAARFIELD, and that the FAARFIELD's designed thickness very likely cannot withstand all of assumed conditions generated within the uncertain variables' ranges.

FAARFIELD does not include all the factors and uncertainty that SOARP considers. Also, FAARFIELD does not optimize over all three design parameters, but SOARP optimizes all three design parameters. By using ANN response models along with the Bayesian simulation optimization, the proposed SOARP method attempts to overcome some of the limitations from which current design methods suffer.

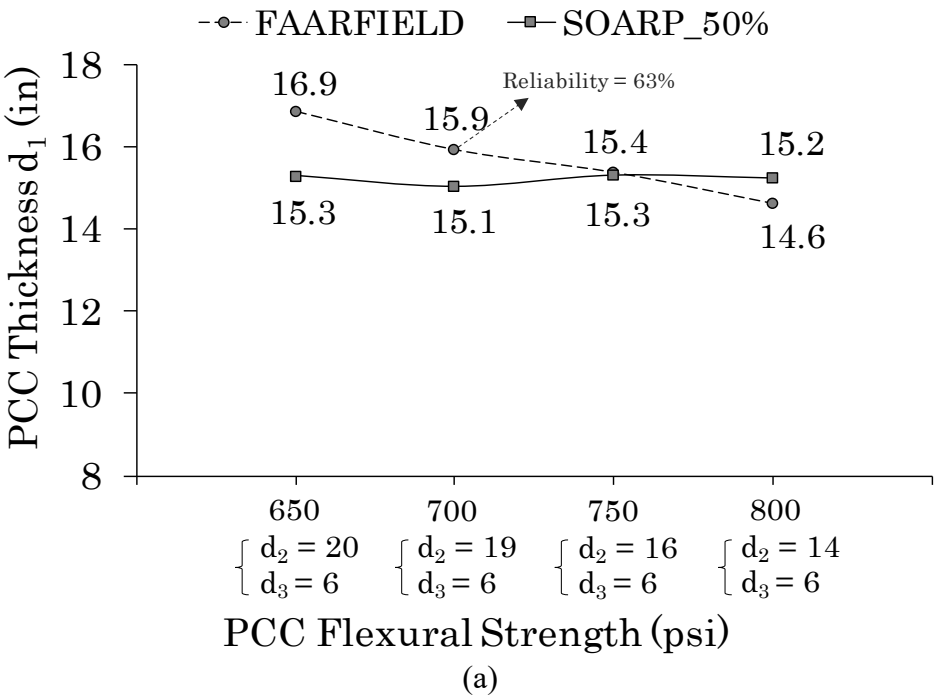

(a)

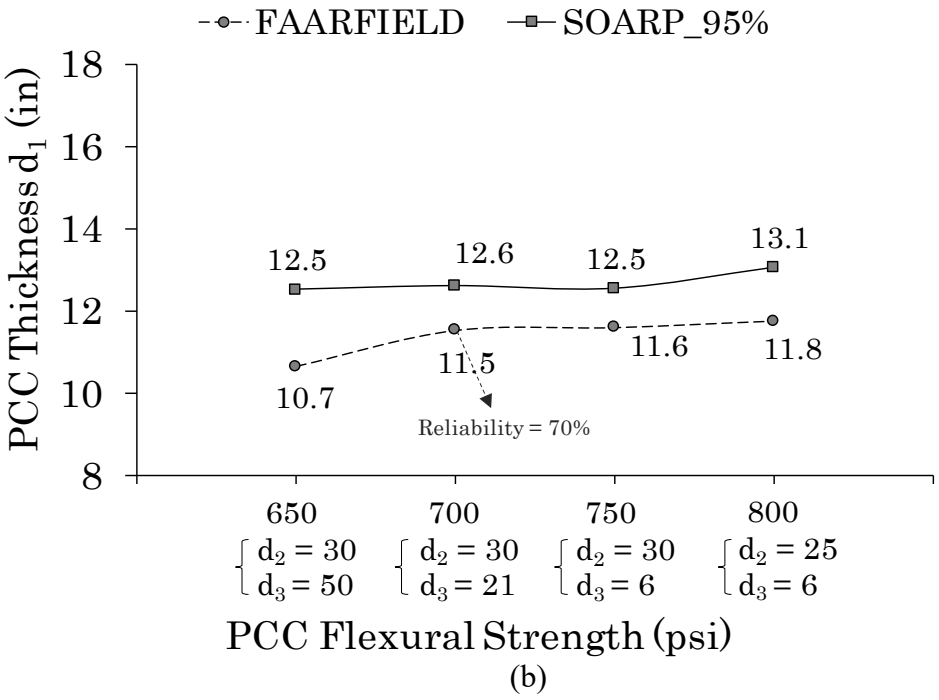

(b)

Figure 5.9 *Comparison of FAARFIELD results and SOARP (a) 50% reliability level (b) 95% reliability level for different flexural strength of the PCC.*

Summary and conclusions

This chapter describes the development of a comprehensive reliability-based simulation-optimization framework for finding the optimal design of airfield concrete pavement consisting of a nine-slab concrete pavement with base and subbase layers atop a subgrade. This study includes aircraft traffic consisting of a B747-8, a B787-8, an A340-500 opt, and an A340-600 opt. Thousands of scenarios were generated to simulate real-world conditions at for long-term usage of the assumed airfield. The design optimization was aimed at minimizing design cost while using a reliability constraint to keep pavement fatigue failure under an allowable amount. In this study ANNs were employed as analysis engines to replicate FEAFAA/NIKE3D-FAA pavement-response solution. Replicating critical stress responses associated with in airfield rigid pavement cracking would significantly make the design process more efficient by reducing total iteration time for calculation of critical responses for each type of aircraft in mixed-aircraft traffic loading.

The design optimization framework was optimized for multiple values of design life (20, 25, and 30 years) and multiple reliability levels (0.5, 0.8, 0.9, and 0.95). The results show that the expected design cost and optimal total thickness produced by 10,000 simulations of the inputs increased while the reliability level and design life increased. For a 80% reliability level and a 20-year design life, the expected cost is $12,310 per slab for a total thickness of 43.4, while for a 95% reliability level and 30-year design life, the total thickness is 49.7 in. It should be noted that by considering thousands of scenarios with uncertain inputs (e.g., loading position of the aircraft), and by estimating the critical stress level using ANN, the pavement structure with the calculated optimum thicknesses should withstand applied traffic and environmental loading during its design life without reaching the maximum fatigue damage level caused by the loading.

We also compared the optimal design found by SOARP with a FAARFIELD design that assumes default thicknesses for the base and subbase layers and then finds slab thickness using iteration, continuing the process until the CDF value becomes 1. In the SOARP framework, we first generated thousands of scenarios of pavement structure and loading conditions and calculated CDF values and an estimation of their distribution. By considering the uncertainty of inputs in CDF calculation, in contrast to FAARFIELD, a designer can simulate possible potential critical conditions. The results show that SOARP either results in more reliable or less expensive pavement designs.

References

[1] FAA, "150/5320-6F - Airport Pavement Design and Evaluation," U.S. Department of Transportation, Washington DC., 2016.

[2] A. Rezaei-Tarahomi, O. Kaya, H. Ceylan, K. Gopalakrishnan, S. Kim, and D. R. Brill, "Neural networks based prediction of critical responses related to top-down and bottom-up cracking in airfield concrete pavements," 2017.

[3] O. Kaya, A. Rezaei-Tarahomi, H. Ceylan, K. Gopalakrishnan, S. Kim, and D. R. Brill, "Developing Rigid Airport Pavement Multiple-Slab Response Models 2 for Top-Down Cracking Mode using Artificial Neural Networks 3," 2017.

[4] A. Rezaei-Tarahomi, O. Kaya, H. Ceylan, S. Kim, K. Gopalakrishnan, and D. R. Brill, "Development of rapid three-dimensional finite-element based rigid airfield pavement foundation response and moduli prediction models," Transp. Geotech., vol. 13, pp. 81–91, 2017.

[5] A. Rezaei-Tarahomi, H. Ceylan, K. Gopalakrishnan, S. Kim, O. Kaya, and D. R. Brill, "Artificial Neural Network Models for Airport Rigid Pavement Top-Down Critical Stress Predictions: Sensitivity Evaluation," in 2019 ASCE International Airfield and Highway Pavements Conference, 2019.

[6] A. Rezaei-Tarahomi, O. Kaya, H. Ceylan, K. Gopalakrishnan, S. Kim, and D. R. Brill, "Neural networks prediction of Critical Responses Related to Top-Down and Bottom-Up Cracking in Airfield Concrete Pavement," in 10th International Conference on the Bearing Capacity of Roads, Railways and Airfields, 2017.

[7] Gaurav, S. F. Wojtkiewicz, and L. Khazanovich, “Optimal design of flexible pavements using a framework of DAKOTA and MEPDG,” Int. J. Pavement Eng., vol. 12, no. 02, pp. 137–148, 2011.

[8] J. Santos and A. Ferreira, “Pavement design optimization considering costs and preventive interventions,” J. Transp. Eng., vol. 138, no. 7, pp. 911–923, 2011.

[9] J. Mikolaj, L. Remek, and M. Macula, “Asphalt Concrete Overlay Optimization Based on Pavement Performance Models,” Adv. Mater. Sci. Eng., vol. 2017, 2017.

[10] M. N. S. Hadi and Y. Arfiadi, “Optimum rigid pavement design by genetic algorithms,” Comput. Struct., vol. 79, no. 17, pp. 1617–1624, 2001.

[11] M. S. Mamlouk, J. P. Zaniewski, and W. He, “Analysis and design optimization of flexible pavement,” J. Transp. Eng., vol. 126, no. 2, pp. 161–167, 2000.

[12] M. Li, M. Sadoughi, C. Hu, Z. Hu, A. T. Eshghi, and S. Lee, “High-Dimensional Reliability-Based Design Optimization Involving Highly Nonlinear Constraints and Computationally Expensive Simulations,” J. Mech. Des., vol. 141, no. 5, p. 51402, 2019.

[13] M. Sadoughi, M. Li, and C. Hu, “Multivariate system reliability analysis considering highly nonlinear and dependent safety events,” Reliab. Eng. Syst. Saf., vol. 180, pp. 189–200, 2018.

[14] D. H. Timm and D. E. Newcomb, “Perpetual pavement design for flexible pavements in the US,” Int. J. Pavement Eng., vol. 7, no. 2, pp. 111–119, 2006.

[15] A. Noshadravan, M. Wildnauer, J. Gregory, and R. Kirchain, “Comparative pavement life cycle assessment with parameter uncertainty,” Transp. Res. Part D Transp. Environ., vol. 25, pp. 131–138, 2013.

[16] E.-B. Lee and C. W. Ibbs, “Computer simulation model: Construction analysis for pavement rehabilitation strategies,” J. Constr. Eng. Manag., vol. 131, no. 4, pp. 449–458, 2005.

[17] C. A. MacKenzie and C. Hu, “Decision making under uncertainty for design of resilient engineered systems,” Reliab. Eng. Syst. Saf., 2018.

[18] Y. Dinegdae, I. Onifade, B. Birgisson, R. Lytton, and D. Little, “Towards a Reliability-Based Pavement Design using Response Surface Methods,” Transp. Res. Rec., p. 0361198118783163, 2018.

[19] I. E. C. D. ARA, “Guide for Mechanistic-Empirical Design OF NEW AND REHABILITATED PAVEMENT STRUCTURES,” Transportation Research Board of the National Academies, Washington D.C., 2003.

[20] P. Dalla Valle, “Reliability in pavement design,” University of Nottingham, 2015.

[21] J. Q. Retherford and M. McDonald, “Reliability Methods Applicable to Mechanistic--Empirical Pavement Design Method,” Transp. Res. Rec., vol. 2154, no. 1, pp. 130–137, 2010.

[22] M. Sanchez-Silva, O. Arroyo, M. Junca, S. Caro, and B. Caicedo, “Reliability based design optimization of asphalt pavements,” Int. J. Pavement Eng., vol. 6, no. 4, pp. 281–294, 2005.

[23] D. R. Brill, Calibration of FAARFIELD Rigid Pavement Design Procdure. Federal Aviation Administration William J. Hughes Technical Center, 2010.

[24] I. Kawa, “Pass-to-Coverage Computation for Arbitrary Gear Configurations in the FAARFIELD Program,” 2012.

[25] FAA, “Airport Pavement Design and Evaluation. AC 150/5320-6F,” 2016.

[26] D. R. Brill and I. Kawa, “Advances in FAA Pavement Thickness Design Software: FAARFIELD 1.41,” in Airfield and Highway Pavements 2017, 2017, pp. 92–102.

[27] Z. Zhang et al., “Opening the black box of neural networks: methods for interpreting neural network models in clinical applications,” Ann. Transl. Med., vol. 6, no. 11, 2018.

[28] C. Thornton, F. Hutter, H. H. Hoos, and K. Leyton-Brown, “Auto-WEKA: Combined selection and hyperparameter optimization of classification algorithms,” in Proceedings of the 19th ACM SIGKDD international conference on Knowledge discovery and data mining, 2013, pp. 847–855.

[29] J. Snoek, H. Larochelle, and R. P. Adams, “Practical bayesian optimization of machine learning algorithms,” in Advances in neural information processing systems, 2012, pp. 2951–2959.

[30] D. J. Lizotte, Practical bayesian optimization. University of Alberta, 2008.

[31] E. Brochu, V. M. Cora, and N. De Freitas, “A tutorial on Bayesian optimization of expensive cost functions, with application to active user modeling and hierarchical reinforcement learning,” arXiv Prepr. arXiv1012.2599, 2010.

[32] P. I. Frazier, “A tutorial on Bayesian optimization,” arXiv Prepr. arXiv1807.02811, 2018.

[33] A. Klein, S. Falkner, S. Bartels, P. Hennig, and F. Hutter, “Fast bayesian optimization of machine learning hyperparameters on large datasets,” arXiv Prepr. arXiv1605.07079, 2016.

[34] Z. Wang, M. Zoghi, F. Hutter, D. Matheson, and N. De Freitas, “Bayesian optimization in high dimensions via random embeddings,” in Twenty-Third International Joint Conference on Artificial Intelligence, 2013.

[35] W. S. P. | P. Brinckerhoff, “Bid Tabulation for Reconstruction of Runway 13-31 Phase 1,” 2016.